Visible light-assisted synthesis of Pt/Bi_2WO_6 and photocatalytic activity for ciprofloxacin

Yafan Wu[1], Xian Zhang[2], Gehong Zhang[1], Weisheng Guan[1]

[1]*School of Environmental Science and Engineering, Chang'an University, Xi'an 710054, People's Republic of China*
[2]*State Key Laboratory of Environmental Chemistry and Ecotoxicology, Research Center for Eco-Environmental Sciences, Chinese Academy of Sciences, Beijing 100085, People's Republic of China*
E-mail: guanweisheng@263.net

Published in Micro & Nano Letters; Received on 30th November 2013; Accepted on 15th January 2014

The Pt/Bi_2WO_6 composite photocatalyst has been successfully synthesised via a photodeposition method. The morphology and the structure of the Pt/Bi_2WO_6 composite samples are characterised by X-ray diffraction, scanning electron microscopy, transmission electron microscopy and UV–vis diffused reflectance spectra. Also discussed are the photocatalytic activities of the obtained samples with different amounts of Pt by investigating the degradation of ciprofloxacin under a Xenon lamp irradiation and it is found that the Pt/Bi_2WO_6 sample with a 1.0 wt% Pt has the highest photocatalytic activity, which is two times of that compared with the pure Bi_2WO_6. Furthermore, the photocatalytic mechanism of the above degradation has been studied.

1. Introduction: With the development of attitudes in society, antibiotics, such as ciprofloxacin (CIP), have been widely used in the cure of humans and animals. To date, a large amount of antibiotics have been detected in soils and in the water in lakes, which would pose a great threat to the environment and human health. Hence, studies on the degradation of antibiotics are important and urgent [1, 2]. There are several methods to deal with the antibiotics existing in the environment, such as adsorption, biology, chemistry and advanced oxidation [3]. The photocatalytic method, as one of the advanced oxidation methods, is widely used to oxidise and degrade different materials in the environment, especially is it is simple, environmentally-friendly and low-cost.

Bi_2WO_6, as an important semiconductor, has been considered one of the promising materials for photocatalysis [4, 5]. However, a problem exists concerning the combination of the photogenerated electrons and the holes of Bi_2WO_6, which seriously affects the photocatalytic activity. To enhance the photoinduced electron-transfer efficiency and decrease the possibility of the combination of photo-generated electrons and holes, precious metals loading is one of the effectively enhanced photocatalytic activities of the materials measures [6, 7]. For example, Zhao *et al.* [8] have synthesised Pt/TNT which was proven to have a better photocatalytic effect compared with P25 in the degradation of methyl orange (MO). Ge [9] has prepared the $Pt/BiVO_4$ to degrade the MO and found that the $Pt/BiVO_4$ has a better photocatalytic ability compared with the bare $BiVO_4$. Teoh *et al.* [10] have reported that the deposited Pt on TiO_2 could enhanced the ability of the photocatalytic activity of methanol, but the Pt(IV) would be decreased. The previous reports have shown that precious metals deposition to improve the photocatalyst activity is related to the species of noble metal and valence and so on.

In this Letter, a simple, ecofriendly and controllable hydrothermal synthetic approach of the three-dimensional (3D) Pt/Bi_2WO_6 structures is reported. We have prepared Pt/Bi_2WO_6 with an advanced photocatalytic performance through the photodeposition method. To the best of our knowledge, this is the first time there has been a synthesis of the Pt doped on the nest-like Bi_2WO_6 and a degradation of the antibiotic (CIP). Furthermore, the catalytic mechanism of the Pt/Bi_2WO_6 is preliminarily studied.

2. Experimental

2.1. Material and methods: $Bi(NO_3)_3{\cdot}5H_2O$, $Na_2WO_4{\cdot}2H_2O$, Na_2SO_4 and $H_2PtCl_6{\cdot}6H_2O$ were of analytical grade and used without further purification; the water used was deionised.

A nest-like Bi_2WO_6 was successfully prepared via the hydrothermal synthesis according to the previous literature [11]. The synthesis of the Pt/Bi_2WO_6 structure: Bi_2WO_6 and $H_2PtCl_6{\cdot}6H_2O$ (0.5, 1.0, 2.0, 3.0 and 5.0 wt%, respectively) were dispersed into the ethanol and transferred into the photochemical reactor. Then, the photodeposition was performed under UV light in the N_2 atmosphere with a vigorous magnetic stirring. After stirring for 2 h, the obtained Pt/Bi_2WO_6 samples with different amounts of the Pt were washed with deionised water and absolute ethanol three times, respectively, and dried in vacuum at 60°C for 6 h.

2.2. Characterisation and measurements: The products were characterised by X-ray diffraction measurements performed on an X-ray diffractometer (XRD, Bruker D8 Advance diffractometer) with Cu-Ka radiation in the range of 10–80° at a scanning rate of $7°min^{-1}$. The morphology of the products was observed by a scanning electron microscopy (SEM, S-4800) and a transmission electron microscope (TEM, JEM-2100). The UV–vis diffused reflectance spectra of the samples were obtained from a UV–vis spectrophotometer (UV2550, Shimadzu, Japan), $BaSO_4$ was used as a reflectance standard. The investigation of the surface of the sample was by an X-ray photoelectron spectrometer (XPS, PHI-5300). Raman spectra were recorded on a Raman spectrometer (WITEC Spectra Pro 2300I) operating with a 532 nm laser. Total organic carbon (TOC) analyses were conducted on a multiN/C2100 (Analytik Jena AG, Germany) TOC analyser.

2.3. Photocatalytic degradation of the antibiotic (CIP): Studies of the photocatalytic properties of the powders were performed at 298 K in our house-made instruments. At first, the photocatalytic activities of the Pt/Bi_2WO_6 powders were evaluated by degradation of the tetracycline antibiotic under visible light irradiation (150 W–Xenon). A 150 W Xenon lamp inside a cylindrical quartz reactor with a circulating water jacket was used as the light source. During the reaction, water was introduced through the jacket to cool the solution. The photochemical reactor contains a 0.1 g catalyst and a 100 ml 10 mg/l tetracycline aqueous solution. The solution was magnetically stirred acutely.

After 30 min in the dark, it reached the absorption balance and its initial absorbency was determined. Then, the solution was irradiated by visible light and was aerated. The sampling analysis was conducted in 10 min intervals. The CIP absorption concentration was determined by using the TU-1800 UV–vis spectrophotometer (Shanghai AoXi Technology Instrument Co., Ltd) by recording the variations of the absorption band maximum at $\lambda = 278$ nm (CIP). The photocatalytic degradation rate (DR) was calculated by the following formula

$$\mathrm{DR} = \left[(1 - A_i/A_0)\right] \times 100\%$$

where A_0 is the initial absorbency of the tetracycline antibiotic waster solution which reached the absorbency balance and A_i is the absorbency of the reaction solution.

3. Results and discussion: The phase purity of the as-synthesised Pt/Bi_2WO_6 samples was characterised by X-ray diffraction (XRD, Fig. 1). All the peaks displayed in the XRD patterns can be readily indexed to a monoclinical phase of the Bi_2WO_6 which are in agreement with the literature values (JCPDS 73-1126). There existed sharp diffraction peaks, which lay at 28.3°, 32.8°, 47.2° and 55.8°, corresponding to the (113), (200) (020), (026) (220) and (313) (208) directions, respectively. In addition, the strong and sharp diffraction peaks of the Pt/Bi_2WO_6 with different amounts of Pt indicate that the Pt/Bi_2WO_6 samples obtained via our simple photodeposition synthetic method are still the same with the pure phase (Bi_2WO_6). The probable reason is that the small amounts of the Pt species introduced in the composite samples or the Pt compounds existed as amorphously [12].

The morphology and the size of the product prepared by the procedure described in the Experimental Section were visualised by the SEM images shown in Fig. 2. As can be seen in Figs. 2*a–c*, the as-obtained Bi_2WO_6 products in the reaction system consist almost entirely of relatively uniform micrometer-scale nests with a 1–2 μm diameter and the surface is smooth. As in Fig. 2*b*, we have also found that the morphology and the size have no obvious differences. The samples of the Pt/Bi_2WO_6 are just a surface coating. They have some point on the surface of the Pt/Bi_2WO_6 in Fig. 2*d*.

To determine the chemical state of the elements, an XPS measurement was performed for the Pt/Bi_2WO_6 sample. As shown in Fig. 3, the Bi 4f7/2 and the Bi 4f5/2 peaks of the Pt/Bi_2WO_6 appear at 159.28 and 164.45 eV, respectively. The W4f7/2 and the O1s feature of the Pt/Bi_2WO_6 are 36.20 and 531.92 eV, respectively. These above results are in agreement with the conventional Bi_2WO_6 nanomaterials [13]. In addition, the peak of 75.45 eV is a response to the Pt4f and indirectly indicates that the Pt exists in the surface of the sample [14].

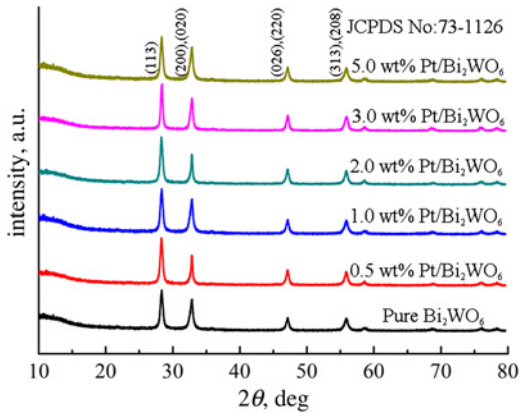

Figure 1 *XRD patterns of the as-obtained samples*

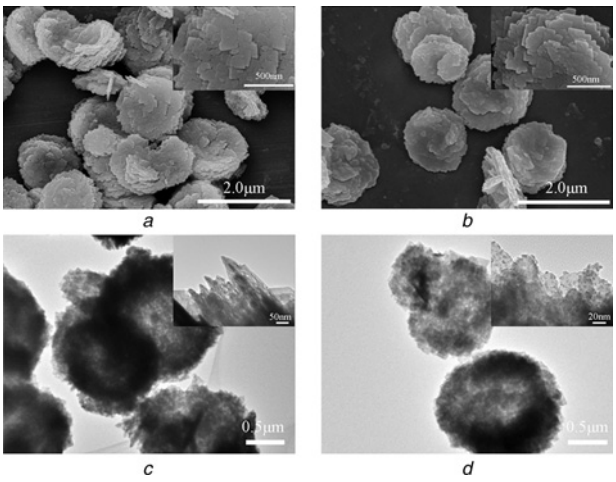

Figure 2 *SEM and TEM images of the pure Bi_2WO_6 and the 1 wt% Pt/Bi_2WO_6 samples*
a and *b* SEM images
c and *d* TEM images

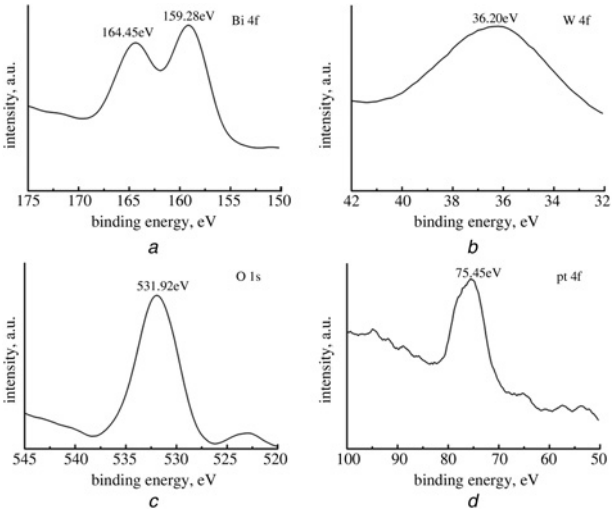

Figure 3 *XPS spectra of the Pt/Bi_2WO_6*
a Bi4f
b W4f
c O1s
d Pt4f

Fig. 4 shows the Raman spectra of the as-obtained Bi_2WO_6 and Pt/Bi_2WO_6 at room temperature. The peak of 150 cm^{-1} is owing to the $[WO_6]^{2-}$, the existence of the peaks in 600–1000 cm^{-1} is due to the W–O stretching mode, 300–310 cm^{-1} may be attributed to the vibrational stretching mode of Bi^{3+} and $[WO_4]^{2-}$, 790–820 cm^{-1} are maybe the symmetric and the antisymmetric vibration peaks of O–W–O [15]. In addition, we can also find that the main peaks of the Bi_2WO_6 are consistent with the 1 wt% Pt/Bi_2WO_6. The decrease in the intensity further indicates that the Pt modified samples on the surface are weakened because of the light signal received by the photocomposite [16].

As shown in Fig. 5, we have studied the UV–vis diffused reflection spectra. The as-obtained Pt/Bi_2WO_6 sample has a obvious absorbency at >400 nm compared with the bare Bi_2WO_6. It had absorption edges at about 450 and 500 nm, respectively, corresponding to the absorption edge of the photocatalyst. The bandgap (E_g) of the photocatalyst is estimated by the

doi: 10.1049/mnl.2013.0705

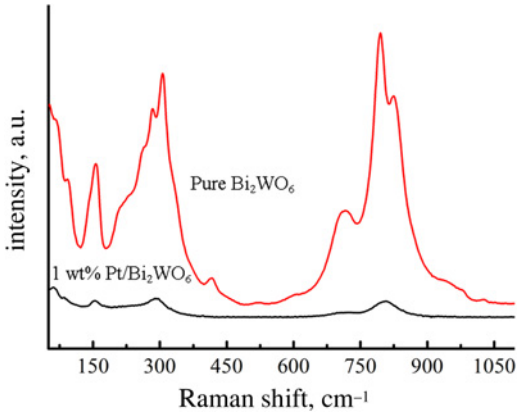

Figure 4 *Raman spectra of the bare Bi_2WO_6 and the 1 wt% Pt/Bi_2WO_6 samples*

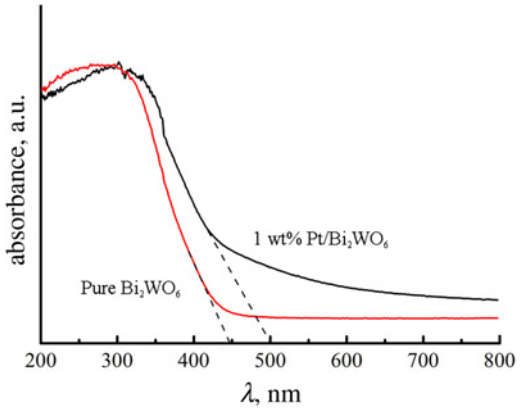

Figure 5 *UV–vis diffused absorption spectra of the bare Bi_2WO_6 and the 1 wt% Pt/Bi_2WO_6 samples*

following equation

$$E_g = 1240/\lambda$$

where λ is the absorbance wavelength.

According to the calculation results, the calculated bandgap energy of the Pt/Bi_2WO_6 photocatalyst is about 2.48 eV, which is much smaller than 2.75 eV (bare). A narrow bandgap of the Pt/Bi_2WO_6 is favourable for absorbing the visible-light as well as the UV-light for the excitation of the electrons from the valence band (VB) to the conduction band. In addition, it can utilise the solar energy more effectively. We have known that the VB level

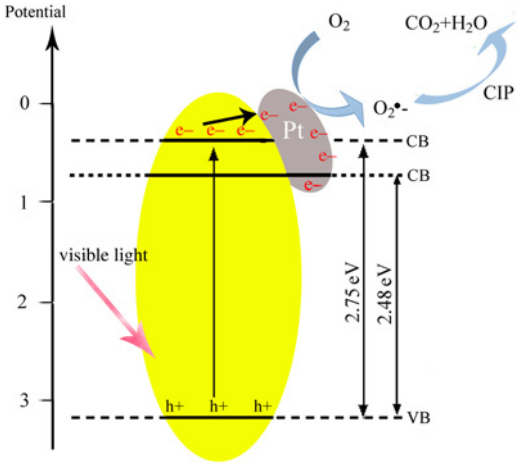

Figure 7 *Postulated mechanism of the photoinduced charge separation of the Pt/Bi_2WO_6*

Bi_2WO_6 is lower by 0.353 V than that of TiO_2. We calculated the $E_{VB} = 0.51$ eV and the $E_{CB} = 3.26$ eV, respectively, for the nest-like Bi_2WO_6 [17].

Therefore the photocatalytic activities of the obtained Pt/Bi_2WO_6 samples were evaluated by the degradation of CIP in water under the visible light irradiation. Fig. 6*a* displays the time-dependent degradation of CIP by the different Pt/Bi_2WO_6 samples under the same photocatalytic degeneration condition. The photocatalytic degeneration rate of the bare Bi_2WO_6 is 35% and the Pt/Bi_2WO_6 (1 wt %) has the best effect of the photocatalytic degeneration. Moreover, in the beginning, with the increase of the loading amount of the Pt on the surface of the Bi_2WO_6, the degeneration rate was enhanced, but with a further increase in the loading amount of the Pt, the photocatalytic degeneration rate decreased.

The main course is deduced as follows. At the beginning, the loading Pt could increase the possibility of the capture of the electrons and thus increase the photocatalytic efficiency. However, with the increase in the amount of the Pt, the Pt will be conglutinated with each other on the surface of the Bi_2WO_6 and thus easily cause the accumulation of the electrons and increase the possibility of the capture of the holes. Therefore these will form the centre of the combination of the electron–holes and decrease the photocatalytic degeneration rate [18].

TOC analysis is an effective method to demonstrate the mineralisation of organic pollutants. Fig. 6*b* shows the degradation of the organic carbon content with Bi_2WO_6 and 1 wt% Pt–Bi_2WO_6 as the photocatalysts; the TOC values are decreased with the irradiation time. Their conversion rates are ca. 60.8% and 23.3% in 60 min, respectively. It has successfully removed the effect of the physical adsorption and correctly evaluated the photocatalytic

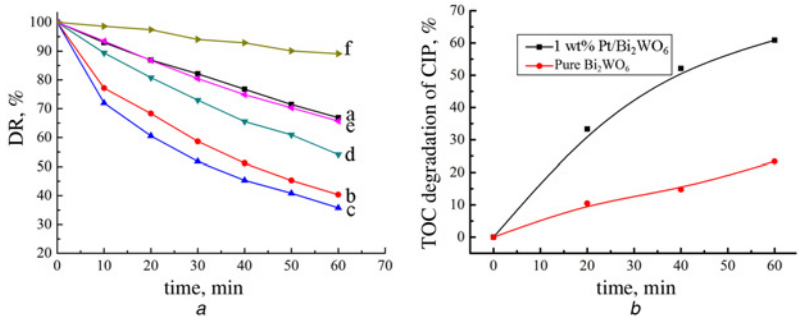

Figure 6 *Photocatalytic degradation of CIP with different Pt/Bi_2WO_6 samples under a visible light irradiation*
a Time dependant degradation of CIP by different $Pt/Bi_2/WO_6$ samples under the same photocatalytic degeneration conditon traces: a pure Bi_2WO_6; b 0.5 wt% Pt/Bi_2WO_6; c 1.0 wt% Pt/Bi_2WO_6; d 2.0 wt% Pt/Bi_2WO_6; e 3.0 wt% Pt/Bi_2WO_6; f 5.0 wt% Pt/Bi_2WO_6
b The TOC of the pure Bi_2WO_6 and the 1 wt% Pt–Bi_2WO_6 samples after the degradation of CIP

activity of the pure Bi_2WO_6 and the 1 wt% Pt–Bi_2WO_6 samples. This result is similar to the trend in the degradation of CIP.

As is well known, one of the most active metals for photocatalytic enhancement is platinum (Pt), which can produce the highest Schottky barrier among the metals that facilitate electron capture [12]. In this reported work, the photocatalytic reaction process was established so that conduction band electrons (e^-) and valence band holes (h^+) are generated when the aqueous Pt/Bi_2WO_6 composite suspension is irradiated with visible light. The recombination of the electrons and the holes must be prevented as much as possible if a photocatalytic reaction is to be favoured. In the photocatalysis system, the photogenerated electrons could react with the electron acceptors such as O_2 existing in the system, reducing it to the superoxide radical anion $\bullet O_2^-$. Thus, the transfer of the charge carriers was improved and the recombination of the electrons and the holes was also inhibited. However, the degradation of CIP cannot be caused either by the effect of $\bullet O_2^-$ directly, or the free $\bullet$OH radicals, because the standard redox potential of Bi(V)/Bi(III) (+1.59 V) is more negative than that of $\bullet OH/OH^-$ (+1.99 V), suggesting that the photogenerated hole on the surface of the Bi_2WO_6 could not react with OH^-/H_2O to form $\bullet$OH [19]. In addition, the Pt/Bi_2WO_6 assisted photodegradation of CIP occurs via two competitive processes: a photocatalytic process and a photosensitised process. Both the photocatalytic process and the photosensitised process would work concurrently under a visible light irradiation, but the former is the predominant process. The visualised photocatalytic mechanism of the Pt/Bi_2WO_6 is shown in Fig. 7.

4. Conclusion: We have successfully synthesised the 3D nest-like Pt/Bi_2WO_6 structure by a simple, ecofriendly and controllable hydrothermal synthetic approach. In addition, we have studied the W–O active modes and the surface of the Pt/Bi_2WO_6 by the Raman and the XPS measures. Moreover, we have studied the effect of the photocatalytic degradation of CIP and found that the loading amount of Pt plays a key role in controlling the photocatalytic degradation activity of CIP. We have also preliminarily studied the catalytic mechanism of the Pt/Bi_2WO_6.

5. Acknowledgments: The authors acknowledge the financial support of the National Natural Science Foundation of China (no. 21007084), the National Basic Research Program of China (2003CB415006), the Knowledge Innovation Program of the Chinese Academy of Sciences (KZCX2-YW-JS406) and the Doctor Foundation (grant no. 20110205110014).

6 References

[1] Baquero F., Martınez J.L., Canton R.: 'Antibiotics and antibiotic resistance in water environments', *Curr. Opin. Biotechnol.*, 2008, **19**, pp. 260–265

[2] Jiao S.J., Zheng S.R., Yin D.Q., Wang L.H., Chen L.Y.: 'Aqueous photolysis of tetracycline and toxicity of photolytic products to luminescent bacteria', *Chemosphere*, 2008, **73**, pp. 377–382

[3] Vasconcelos T.G., Henriques D.M., König A., Martins A.F., Kümmerer K.: 'Photo-degradation of the antimicrobial ciprofloxacin at high pH: identification and biodegradability assessment of the primary by-products', *Chemosphere*, 2009, **76**, pp. 487–493

[4] He Z., Sun C., Yang S.G., Ding Y.C., He H., Wang Z.L.: 'Photocatalytic degradation of rhodamine B by Bi_2WO_6 with electron accepting agent under microwave irradiation: mechanism and pathway', *J. Hazard Mater.*, 2009, **162**, pp. 1477–1486

[5] Lee W.L.W., Huang S.T., Chang J.L., Chen J.Y., Cheng M.C., Chen C.C.: 'Photodegradation of CV over nanocrystalline bismuth tungstate prepared by hydrothermal synthesis', *J. Mol. Catal. A, Chem.*, 2012, **361–362**, pp. 80–90

[6] Kumar R.V., Raza G.: 'Photocatalytic disinfection of water with Ag-TiO_2 nanocrystalline composite', *Ionics*, 2009, **15**, pp. 579–587

[7] Wu Z.B., Sheng Z.Y., Liu Y., Wang H.Q., Tang N., Wang J.: 'Characterization and activity of Pd-modified TiO_2 catalysts for photocatalytic oxidation of NO in gas phase', *J. Hazard Mater.*, 2009, **164**, pp. 542–548

[8] Zhao Q., Li M., Chu J.Y.: 'Preparation, characterization of Au (or Pt)-loaded titania nanotubes and their photocatalytic activities for degradation of methyl orange', *Appl. Surf. Sci.*, 2009, **255**, pp. 3773–3778

[9] Ge L.: 'Novel visible-light-driven Pt/$BiVO_4$ photocatalyst for efficient degradation of methyl orange', *J. Mol. Catal. A, Chem.*, 2008, **282**, pp. 62–66

[10] Teoh W.Y., Mädler L., Amal R.: 'Inter-relationship between Pt oxidation states on TiO_2 and the photocatalytic mineralisation of organic matters', *J. Catal.*, 2007, **251**, pp. 271–280

[11] Yan Y., Wu Y.F., Yan Y.T., Guan W., Shi W.: 'Inorganic-salt-assisted morphological evolution and visible-light-driven photocatalytic performance of Bi_2WO_6 nanostructures', *J. Phys. Chem. C*, 2013, **117**, pp. 20017–20028

[12] Duan F., Zheng Y., Chen M.Q.: 'Flowerlike $PtCl_4$/Bi_2WO_6 composite photocatalyst with enhanced visible-light-induced photocatalytic activity', *Appl. Surf. Sci.*, 2011, **257**, pp. 1972–1978

[13] Xiao Q., Zhang J., Xiao C., Tan X.K.: 'Photocatalytic degradation of methylene blue over Co_3O_4/Bi_2WO_6 composite under visible light irradiation', *Catal. Commun.*, 2008, **9**, pp. 1247–1253

[14] Jang J.S., Choi S.H., Kim H.G., Lee J.S.: 'Location and state of Pt in platinized CdS/TiO_2 photocatalysts for hydrogen production from water under visible light', *J. Phys. Chem. C*, 2008, **112**, pp. 17200–17205

[15] Crane M., Frost R.L., Williams P.A., Theo Kloprogge J.: 'Raman spectroscopy of the molybdate minerals chillagite (tungsteinian wulfenite-I4), stolzite, scheelite, wolframite and wulfenite', *J. Raman. Spectrosc.*, 2002, **33**, pp. 62–66

[16] Zhou B., Zhao X., Liu H.J., Qu J.H., Huang C.P.: 'Visible-light sensitive cobalt-doped $BiVO_4$ (Co-$BiVO_4$) photocatalytic composites for the degradation of methylene blue dye in dilute aqueous solutions', *Appl Catal B, Environ.*, 2010, **99**, pp. 214–221

[17] Shang M., Wang W., Zhang L., Sun S.M., Wang L., Zhou L.: '3D Bi_2WO_6/TiO_2 hierarchical heterostructure: controllable synthesis and enhanced visible photocatalytic degradation performances', *J. Phys. Chem. C*, 2009, **113**, pp. 14727–14731

[18] Yu C.L., Yu J.C., Fan C.F., Wen H.R., Hu S.J.: 'Synthesis and characterization of Pt/BiOI nanoplate catalyst with enhanced activity under visible light irradiation', *Mater. Sci. Eng. B*, 2010, **166**, pp. 213–219

[19] Fu H.B., Pan C.S., Yao W.Q., Zhu Y.F.: 'Visible-light-induced degradation of rhodamine B by nanosized Bi_2WO_6', *J. Phys. Chem. B*, 2005, **109**, pp. 22432–22439

doi: 10.1049/mnl.2013.0705